

A 50

Absorption spectra of dyes

08.01.2020

Group 39

Lorenzo Wormer and Louis Kontschak

Supervisor: Yi Luo

Contents

1 Task	1
2 Theoretical Foundations	1
2.1 Cyanine dyes	1
2.2 The particles in a box model for cyanine dyes	3
2.3 Absorption and quantitative analysis	4
3 Methods	6
3.1 Recording the spectrograms	6
3.2 Analysis of spectrogram data	6
3.2.1 Identification of dyes and evaluation of model	6
3.2.2 Estimating concentrations via dipole moment	7
4 Results	10
5 Discussion	12
6 Appendix	14

1 Task

This experiment deals with the determination of the absorption spectra of different cyanine dyes. Whereby light with a wavelength in the range of 400 to 800 nm was used. By means of the results the unknown investigated dyes were characterized.

2 Theoretical Foundations

2.1 Cyanine dyes

Cyanine dyes make up a homologous series with the following general structure:

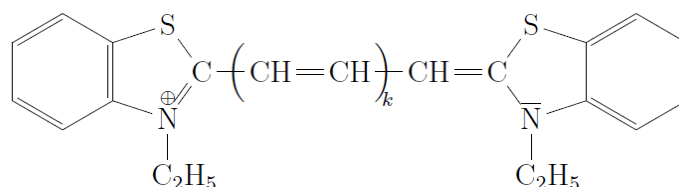


Fig. 1: The general chemical structure of cyanine dyes with $k = 0, 1, 2, 3$. The number of double bonds equals to $j = k + 2$.¹

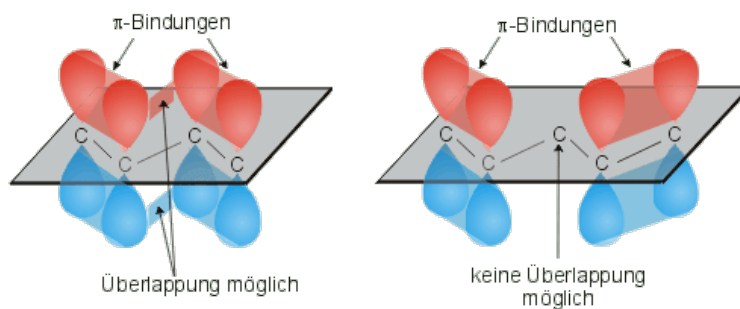


Fig. 2: Delocalisation mechanism of the π -electrons in conjugated double bonds.²

¹ **Source:** Experiment script A50 'Absorption spectra of dyes', Institute for physical chemistry KIT, 2018-01

² **Source:** 'Chemical bonds - Conjugated double bounds' in 'CHEMGAROO - ChemgaPedia', Prof. Dr. Rainer Herges and Kirsten Klose, last downloaded 2020-01-14

The double bonds form a conjugated system in which the π -electrons are delocalized and can move freely. Figure 2 shows the effect of overlapping p-orbitals in conjugated double bonds that leads to the delocalisation of the π -electrons. This effect is responsible for the remarkable light absorbing ability of cyanine dyes. With the 'particle in a box' model the absorption can be described more physically:

2.2 The particles in a box model for cyanine dyes

The particle in a box model can be used for describing the potential curve of electrons within a molecule. For cyanine dyes a realistic potential curve of the π -electrons is given by the red line in figure 3. As one can see the electrons have a potential energy of nearly zero in the area of the conjugated system. At the borders of the conjugated system, in the area of the nitrogen atoms, the potential energy is heading for infinity, because the electron probability density here is practically zero. The real potential curve is approximated by the 'particle in a box' model which is given by the black line in figure 3. The model only differentiates between the states of infinite potential energy and a potential energy of zero. By solving the Schrödinger equation for the movement of an electron in the box we get standing waves with the wave function

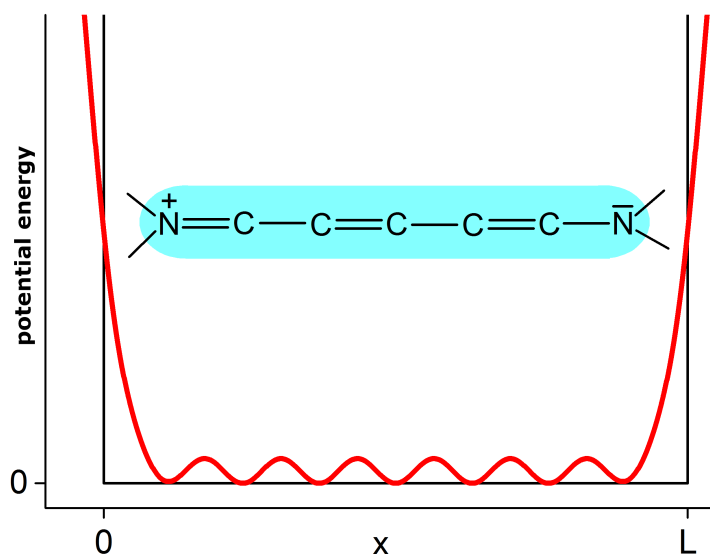


Fig. 3: A realistic potential curve of the π -electrons (red line) and the approximation with the 'particle in a box' model (black line).³

³ **Source:** Experiment script A50 'Absorption spectra of dyes', Institute for physical chemistry KIT, 2018-01

$$\Psi_n(x) = \sqrt{\frac{2}{L}} \sin\left(\frac{n\pi x}{L}\right); \quad n = 1, 2, 3, \dots \quad (1)$$

For the eigen-values of the energy states n (thus the electron probability densities or molecule orbitals) follows:

$$E_n = \frac{h^2}{8mL^2} n^2 \quad (2)$$

Whereby m is the mass of an electron and h the Planck's constant. The smallest amount of energy that is needed to push a molecule in the excited state is the energy difference between the highest occupied molecule orbital (HOMO) and the lowest unoccupied molecule orbital (LUMO). In the absorption spectrum this results in the absorption band at the highest wave length (thus lowest frequency respectively lowest energy). The energy difference between the HOMO and the LUMO is calculated by:

$$\Delta E = E_{LUMO} - E_{HOMO} = \frac{h^2}{8mL^2} (n_{LUMO}^2 - n_{HOMO}^2) \quad (3)$$

To calculate the needed wave length for the HOMO-LUMO transition (that is the maximal wave length in the absorption spectrum) we use equation (4):

$$\lambda_{max} = \frac{hc}{\Delta E} \quad (4)$$

2.3 Absorption and quantitative analysis

The absorption effect can be used for some quantitative analysis, just like the determination of the concentration of a sample: When light enters through a sample in a cell and absorption occurs, the light intensity of the light that leaves the cell differs from the intensity of the light entering the cell. The different intensities are related to the concentration by Lambert-Beer's law:

$$OD(\nu) = \lg \frac{I_0(\nu)}{I(\nu)} = \epsilon(\nu) c_J D \quad (5)$$

Whereby OD is called the optical density of the investigated sample. $I_0(\nu)$ is the entering and $I(\nu)$ the transmitted light intensity. These variables depend on the frequency ν of the entering light. c_J is the required sample concentration and D the length of the cell. The proportionality factor $\epsilon(\nu)$ is

called extinction coefficient and depends again on the frequency of the used light. When plotting the optical density or the extinction coefficient over the frequency or the wave length of the used light one gets the absorption spectrum of the investigated sample.

3 Methods

Four solutions of the cyanine dye compounds *N,N'*-diethyl-2,2'-thiacyanine iodide (DTI), *N,N'*-diethyl-2,2'-dithiacarbocyanine iodide (DTCI), *N,N'*-diethyl-2,2'-dithiadibocarbocyanine iodide (DTDCI) and *N,N'*-diethyl-2,2'-dithiaditricarbocyanine iodide (DTTCI) were received ready-prepared in cuvettes, and the spectrogram of each was subsequently measured and analyzed. The chemical identity of each solution had to be determined through this measurement and thus was not known beforehand, so the four cuvettes were labelled with different symbols: \times (cross), \circ (circle), Δ (triangle) and \square (square).

3.1 Recording the spectrograms

The spectrograms were recorded using the software *Lambda-SPX* on a computer connected to a spectrometer, which was calibrated against the known wavelength a deuterium lamp (652.2 nm). The software was configured to record optical densities (OD_ν), hence the value corresponding to the left side of equation (5). After recording a baseline once without a sample, the spectrogram for each solution was recorded in 1 nm steps starting from a wavelength of 350 nm and ending at 800 nm, by placing the cuvette into the spectrometer and starting an automatic sweep through the preconfigured wavelength-interval. The recorded spectrograms can be found as $OD - \nu$ plots in the appendix.

3.2 Analysis of spectrogram data

3.2.1 Identification of dyes and evaluation of model

For each of the four spectrograms (cross, circle, triangle and square), the wavelength at maximum OD_ν value was determined and denoted with ν_{max} . Through transforming equation (4), the energy ΔE corresponding to each ν_{max} was calculated. This value represents the actual difference between the LUMO and HOMO orbital of the measured cyanine dye, so it was denoted with ΔE_{real} . Table 2 in the results section shows this value for all samples.

The same quantity can also be calculated from the model of a *particle in a box* - as described in the theory section - by employing equation (3). To distinguish, this theoretical energy difference was denoted by ΔE_{model} .

The values n_{HOMO} and n_{LUMO} , needed as input to this equation, can be calculated from the number of conjugate double bonds j via $n_{HOMO} = j + 1$ and $n_{LUMO} = j + 2$. The double bond count itself can be determined from the molecule's structure (see figure 1) via $j = k + 2$, where k is the number of repeating unit cells. The results of this are shown in table 1.

According to the two values ΔE_{real} and ΔE_{model} , which in theory should match, the different cyanine dyes could be associated with the unknown samples. Additionally, through calculating the deviation of ΔE_{real} from ΔE_{model} (by calculating their difference), the accuracy of the employed theoretical model could be assessed.

3.2.2 Estimating concentrations via dipole moment

Another connection between theoretical model and empirical measurement can be made via equation (6). This equation relates the so-called *transition dipole moment* μ_{fi} , which is derived from a quantum-mechanical (QM) model, to the quantity $\epsilon_{max} \cdot \Delta\nu_{half}$, which can be calculated from a measured spectrogram.

$$\epsilon_{max} \cdot \Delta\nu_{half} \approx \int_{\nu_1}^{\nu_2} \epsilon(\nu) d\nu \approx 1.477 \cdot 10^{93} (\text{mol } A^2 \text{ m}^2 \text{ kg s})^{-1} \cdot \Delta E \cdot |\mu_{fi}|^2 \quad (6)$$

ϵ_{max} is the extinction coefficient at the wavelength of the peak ν_{max} and can be calculated from $OD_{\nu_{max}}$ by transforming equation (5), as shown in equation (7). The length d was thereby set to the diameter of the used cuvettes, which was 1 cm, and $c_{assumed}$ was assumed to be $6 \cdot 10^{-6} \frac{\text{mol}}{\text{L}}$.

$$\epsilon_{max} = \frac{OD_{\nu_{max}}}{\nu_{max} \cdot d \cdot c_{assumed}} \quad (7)$$

$\Delta\nu_{half}$ denotes the width of the peak around ν_{max} at half the peak height in the spectrogram and can be determined as shown in figure 4.

For the specific QM model of a particle in a box, μ_{fi} can be calculated approximately according to equation (8), where e denotes the elementary charge and L the length of the potential well.

⁴ **Source:** Experiment script A50 'Absorption spectra of dyes', Institute for physical chemistry KIT, 2018-01

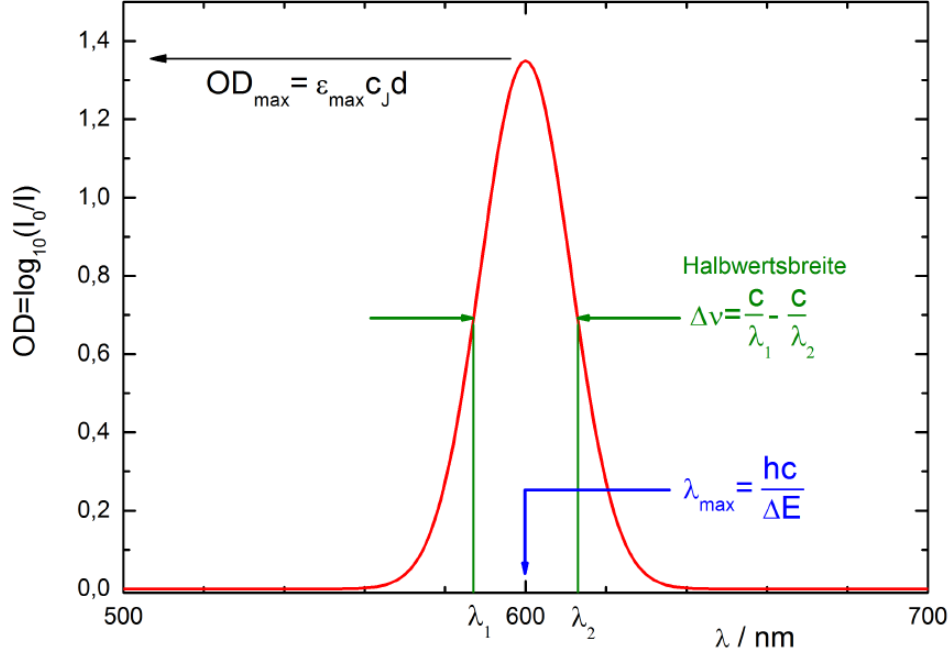


Fig. 4: How to calculate the half width $\Delta\nu_{half}$ of a peak in a spectrogram ⁴

$$\mu_{fi} := \int_{-\infty}^{\infty} \psi_f^* x \psi_i dx \approx -\frac{2eL}{\pi^2} \quad (8)$$

L was calculated from the count of double bonds j (compare to figure 1) and the mean bond length $d = 144 \text{ pm}$ through equation (9).

$$L = (2j + 2)d \quad (9)$$

For the samples labelled with a cross and a square, the value of $\epsilon_{max} \cdot \Delta\nu_{half}$ has been calculated both from the theoretical values of μ_{fi} and ΔE_{model} , which was denoted with the index *model*, and from the measured values of ϵ_{max} and $\Delta\nu_{half}$, denoted with the index *real*.

According to these differing values - and assuming the accuracy of the model - the assumed concentration $c_{assumed}$ was corrected to reflect the real concentration c within the sample via equation (10).

$$c = \frac{(\epsilon_{max} \cdot \Delta\nu_{half})_{model}}{(\epsilon_{max} \cdot \Delta\nu_{half})_{real}} \cdot c_{assumed} \quad (10)$$

The results of all these calculations are shown in table 3.

4 Results

Tables 1 and 2 show the results of the calculations described in method section 3.2.1. The results of the calculations in method section 3.2.2 are listed analogously in table 3. The second row of each table informs about the unit of numerical columns (if any), while the third row references the calculation, which the values originated from.

Tab. 1: ΔE calculated from theoretical model of each compound

Dye	k	j	n_{HOMO}	n_{LUMO}	L	ΔE_{model}
					m	<i>Joule</i>
		$= k + 2$	$= j + 1$	$= j + 2$	Eq. (9)	Eq. (3)
DTI	0	2	3	4	$8.64 \cdot 10^{-10}$	$5.649 \cdot 10^{-19}$
DTCI	1	3	4	5	$1.152 \cdot 10^{-9}$	$4.085 \cdot 10^{-19}$
DTDCI	2	4	5	6	$1.440 \cdot 10^{-9}$	$3.196 \cdot 10^{-19}$
DTTCI	3	5	6	7	$1.728 \cdot 10^{-9}$	$2.623 \cdot 10^{-19}$

Tab. 2: ΔE calculated from spectrogram of each sample

Sample	Symbol	ν_{max}	ΔE_{real}
		nm	Joule
			Eq. (4)
Circle	○	423	$4.696 \cdot 10^{-19}$
Triangle	△	543	$3.658 \cdot 10^{-19}$
Cross	×	652	$3.047 \cdot 10^{-19}$
Square	□	759	$2.617 \cdot 10^{-19}$

Tab. 3: Estimation of concentrations c via dipole moment

Dye	S	μ_{fi}	$(\epsilon_{max} \cdot \Delta\nu_{half})_{model}$	ϵ_{max}	$\Delta\nu_{half}$	$(\epsilon_{max} \cdot \Delta\nu_{half})_{real}$	c
		$A \cdot m \cdot s$	$m^2 \cdot mol^{-1} \cdot s^{-2}$	$m^2 \cdot mol^{-1} \cdot s^{-1}$	nm	$m^2 \cdot mol^{-1} \cdot s^{-2}$	$mol \cdot m^{-3}$
		Eq. (8)	Eq. (6) (left side)	Eq. (7)	Fig. 4	Eq. (6) (right side)	Eq. (10)
DTDCI	\times	$-4.68 \cdot 10^{-29}$	$1.031 \cdot 10^{18}$	13395.76	42	$4.01 \cdot 10^{17}$	0.00233
DTTCI	\square	$-5.61 \cdot 10^{-29}$	$1.219 \cdot 10^{18}$	19866.41	58	$6.09 \cdot 10^{17}$	0.00299

5 Discussion

Combining the results in tables 1 and 2 allows for identifying the dyes contained in all unknown samples by simply matching each value of ΔE_{real} with the closest value of ΔE_{model} . The result of this matching is shown in table 4.

For evaluating the accuracy of the chosen QM model (particle in a box), the difference between theoretical and empirical value of ΔE can be calculated. Normalizing that difference to the empirical value ΔE_{real} yields a relative error, which quantifies the model’s inaccuracy. These two values are also depicted for each sample in table 4.

Tab. 4: Identification of samples and evaluation of model accuracy

Dye	matched sample	$\Delta E_{model} - \Delta E_{real}$	Relative Model Error
		Joule	%
DTI	○	$-9.534 \cdot 10^{-20}$	20.3
DTCI	△	$-4.275 \cdot 10^{-20}$	11.7
DTDCI	×	$-1.493 \cdot 10^{-20}$	4.9
DTTCI	□	$-5.772 \cdot 10^{-22}$	0.2

As can be seen through the relative model error values in table 4, the model gets more accurate with an increasing number of conjugate double bonds. Looking at figure 3 in the theory section, this is to be expected, since the actual potential curve of an electron within the conjugate system will resemble the model of a particle in a box more closely, the longer the conjugate system is, hence the more bonds it has.

Even given that fact though, the extremely small relative error of just 0.2 % for the compound DTTCI is quite remarkable. In order to rule out that this close match has been produced by mere coincidence, further repetitions of this experiment would be advisable.

Given the small relative model errors of both DTDCI and DTTCI, the calculated concentration for the samples of these compounds, as shown in table 3, can be taken to be fairly accurate. Assuming that both samples are

supposed to contain the same concentration of dye, the calculated value of $c = 0.00299 \frac{\text{mol}}{\text{m}^3}$ for the sample of DTTCI is likely the best estimate, as the QM model for DTTCI was the most accurate. Hence, it can fairly reasonably be concluded that the samples provided were diluted to a dye concentration of $3 \cdot 10^{-6} \frac{\text{mol}}{\text{L}}$, rather than the $6 \cdot 10^{-6} \frac{\text{mol}}{\text{L}}$ that were initially assumed.

6 Appendix

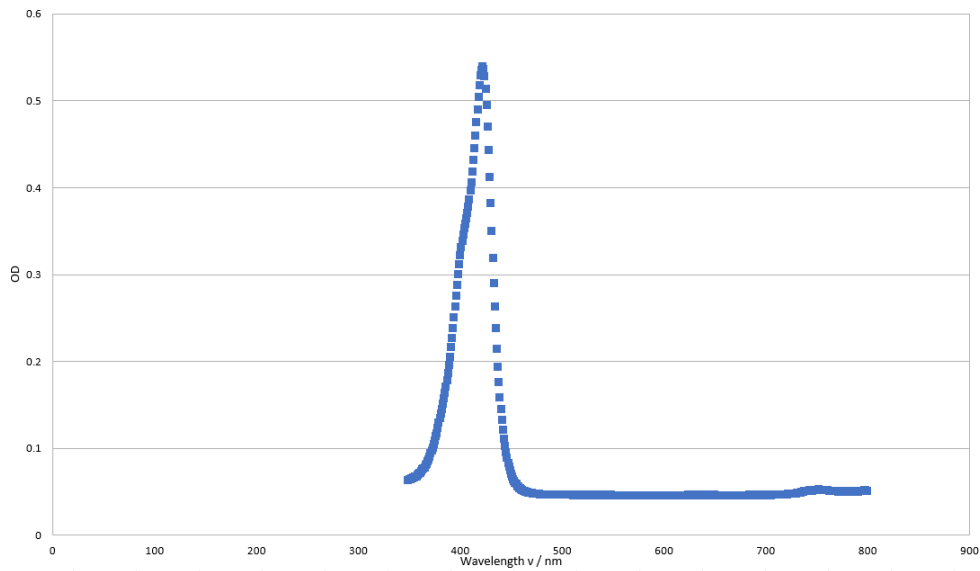


Fig. 5: Spectrogram of the sample labelled with a circle

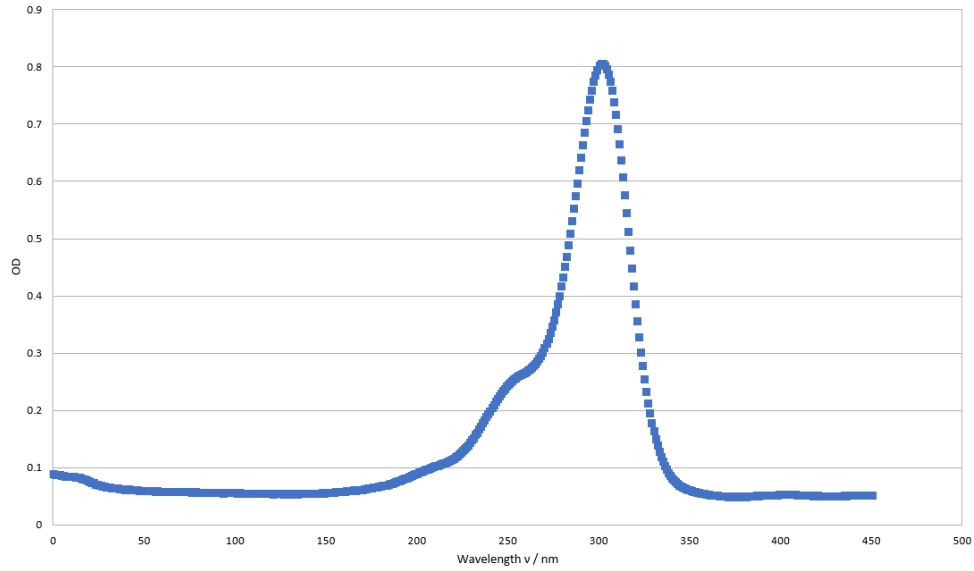


Fig. 6: Spectrogram of the sample labelled with a cross

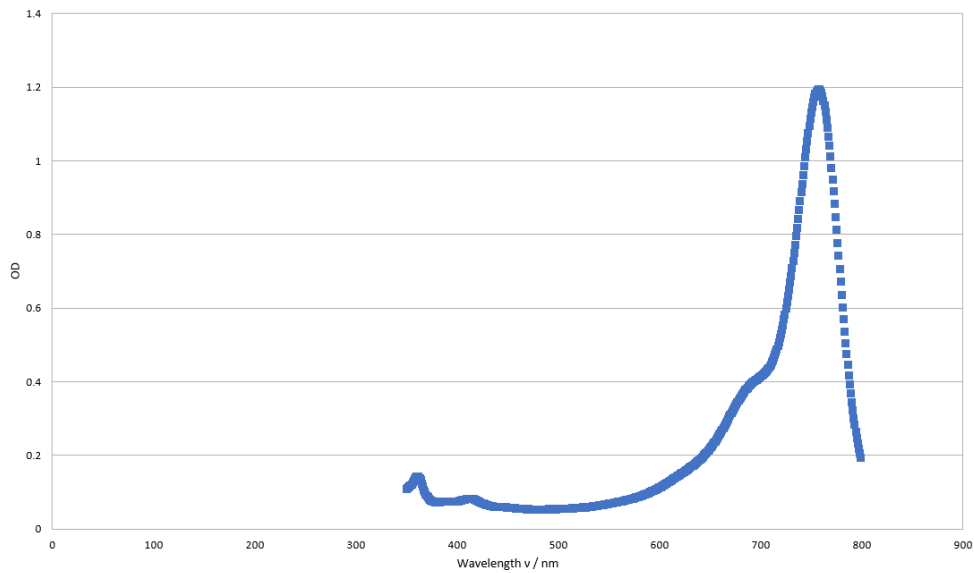


Fig. 7: Spectrogram of the sample labelled with a square

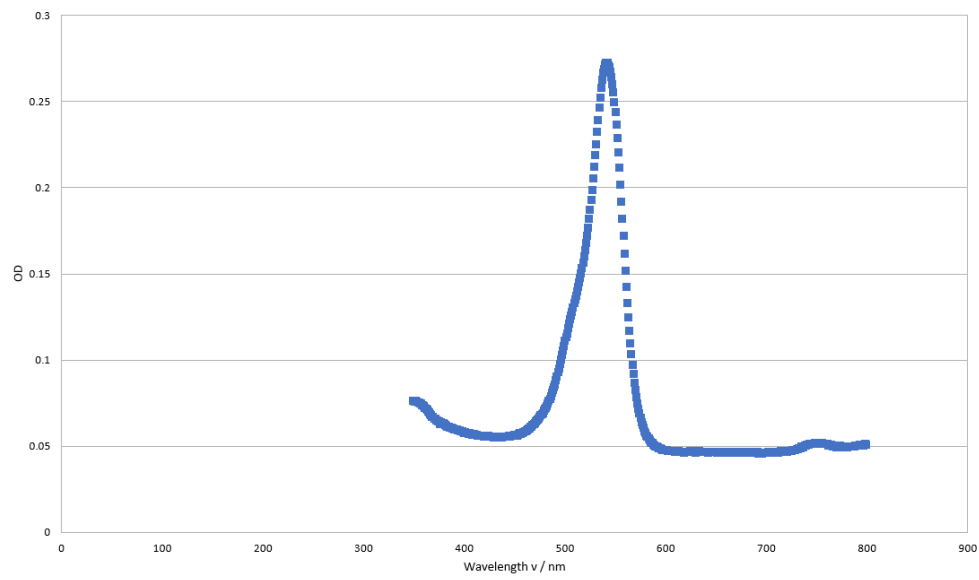


Fig. 8: Spectrogram of the sample labelled with a triangle